

Manuscript for “*British Journal of Clinical Pharmacology*”

Model-informed precision dosing for alemtuzumab in pediatric and young adult patients undergoing allogeneic hematopoietic cell transplantation

Min Dong^{1,3*#}, Chie Emoto^{1,3*}, Tsuyoshi Fukuda^{1,3}, Danielle E. Arnold², Parinda A. Mehta^{2,3}, Rebecca A. Marsh^{2,3}, Alexander A. Vinks^{1,3}

¹)Division of Clinical Pharmacology; ²)Division of Bone Marrow Transplantation and Immune Deficiency, Cincinnati Children’s Hospital Medical Center, Cincinnati, Ohio USA; and

³)Department of Pediatrics, University of Cincinnati College of Medicine, Cincinnati, Ohio USA

*Contributed equally

#Corresponding author:

Min Dong, PhD

Division of Clinical Pharmacology

Cincinnati Children's Hospital Medical Center

3333 Burnet Ave, MLC 6018, Cincinnati, OH, USA

Email: min.dong@cchmc.org

Running head: Alemtuzumab optimal dosing in pediatric patients

Keywords: alemtuzumab, pharmacokinetics, pharmacodynamics, hematopoietic cell transplantation, children, precision dosing

Word count: ~4163

Table count: 3

Figure count: 5 (Supplemental figure count: 5)

Acknowledgement: This work was supported by a Cincinnati Children's Research Foundation GAP award.

Conflicts of Interest: The authors have no conflict of interest to declare.

What is already known about this subject?

- Current off-label use of alemtuzumab results in large variability in drug exposure and response in pediatric patients undergoing allogeneic hematopoietic cell transplantation (HCT).
- Our previous studies have shown that an alemtuzumab concentration of 0.15-0.6 µg/mL on the day of transplantation (Day 0) is associated with better clinical outcomes.

What this study adds?

- An integrated population PK/PD model of alemtuzumab was developed for dose optimization in pediatric and young adult patients undergoing HCT.
- Based on this model, an improved allometry-based or BSA-based starting dose is proposed in combination with individualized PK estimation using alemtuzumab concentration feedback and Bayesian estimation for further study.

ABSTRACT

Aim: Alemtuzumab is a lymphodepleting monoclonal antibody utilized in conditioning regimens for allogeneic hematopoietic cell transplantation (HCT). A therapeutic range of 0.15-0.6 $\mu\text{g/mL}$ on the day of transplantation is associated with better HCT outcomes. The purpose of this study was to characterize alemtuzumab population pharmacokinetic/pharmacodynamic (PK/PD) and to propose individualized subcutaneous dosing schemes to achieve this optimal level for pediatric patients.

Methods: Alemtuzumab concentration and absolute lymphocyte count (ALC) profiles were obtained from 29 patients with non-malignant disorders undergoing HCT. PK/ PD analyses were performed using non-linear mixed effects modeling. Monte Carlo simulation was conducted to evaluate different improved dosing approaches.

Results: A one-compartment model with sequential zero- and first-order absorption adequately described subcutaneously administered alemtuzumab PK. Model fit was significantly improved by including allometrically scaled body weight on clearance (0.080 L/h/70kg) and volume of distribution (17.4 L/70kg). ALC reduction following subcutaneous alemtuzumab was swift. An inhibitory E_{max} model best characterized the relationship between alemtuzumab concentration and ALC. E_{max} and EC_{50} were estimated as $1.18 \times 10^3/\mu\text{L}$ and $0.045\mu\text{g/mL}$, respectively. The currently used per kg dosing was found to cause uneven alemtuzumab exposure across different age and weight cohorts. Simulations indicated optimal target achieving dose as allometry-based of $18 \text{ mg} \cdot (\text{weight}/70)^{0.75}$ or body surface area (BSA)-based of $10 \text{ mg}/\text{m}^2$, divided over 3 days, with a potential individualized top-up dose; both of which yielded similar results.

Conclusion: An allometry- or BSA-based starting dosing regimen in combination with individualized Bayesian PK estimation using concentration feedback is proposed for alemtuzumab precision dosing in children undergoing allogeneic HCT.

Introduction

Alemtuzumab is a humanized monoclonal antibody directed against CD52 with the ability to deplete lymphocytes and other immune cells. It is often used together with fludarabine and melphalan or other chemotherapeutic agents as part of reduced intensity conditioning (RIC) regimens for allogeneic hematopoietic cell transplantation (HCT) [1]. Our group previously reported the impact of peri-transplant alemtuzumab levels on acute graft versus host disease (GVHD), mixed chimerism, and lymphocyte recovery [2]. We found that if alemtuzumab concentrations fell within the range of 0.2-0.4 $\mu\text{g/mL}$ on Day 0, the incidences of GVHD and mixed chimerism were significantly lower. Conversely, concentrations over 0.6 $\mu\text{g/mL}$ on Day 0 were associated with undesired delayed post-transplant immune reconstitutions (IR). Based on these findings, a concentration of 0.15-0.6 $\mu\text{g/mL}$ was proposed as the ideal alemtuzumab exposure target on Day 0. To achieve this target, a reduced alemtuzumab dosing schedule combined with a Bayesian adaptive control strategy was recently applied in a prospective pilot study (Arnold et al., submitted; attached as supplemental materials). This dosing protocol administered a cumulative dose of 0.5-0.6 mg/kg subcutaneously divided over three days starting on Day -14. A pharmacokinetically (PK) guided approach [3] was applied using individual Bayesian estimation and a top-up dose was given if the predicted Day 0 alemtuzumab concentrations were below 0.15 $\mu\text{g/mL}$. This precision dosing strategy led to twice the number of patients achieving the ideal therapeutic range of 0.15-0.6 $\mu\text{g/mL}$ on Day 0 compared to patients who received traditional intermediate alemtuzumab dosing without PK modeling [4]. However, approximately 42% of patients had a Day 0 alemtuzumab concentration still above the target range, suggesting the need for further model-informed dose optimization.

Previous studies report large variability in alemtuzumab PKs in adult [5] and pediatric patients affecting alemtuzumab exposure including Day 0 concentrations [4]. Although targeted alemtuzumab exposure can be achieved by monitoring peri-transplant concentrations after the initial dose and administering additional doses as needed, absolute optimization cannot be achieved without predictive population PK models. Population PK models provide the required average parameter and quantitative estimates of inter-patient variability essential for such precision dosing protocols [6]. Population PK models of alemtuzumab after intravenous administration have been described in adults [5] and recently also in pediatric patients [7]. To date, no formal reports have been published on PK models with subcutaneously administered

101 alemtuzumab, an administration route impacted by multiple factors affecting absorption [8]. In
102 addition, despite a clear inhibitory relationship between alemtuzumab administration and
103 lymphocytes depletion, a quantitative characterization of alemtuzumab concentration versus
104 absolute lymphocytes count (ALC) is lacking. With the goal of identifying an optimal dosing
105 schedule for alemtuzumab in allogeneic HCT, prospective intensive sampling PK and PK-PD
106 studies after subcutaneous alemtuzumab were conducted by our group in pediatric and young
107 adult patients undergoing HCT. Using data collected in these studies, here we intended to: 1)
108 establish a population PK model for alemtuzumab after subcutaneous administration based on
109 our preliminary PK analysis [9] with additional data from a recent pilot study (Clinicaltrials.gov
110 NCT03302754; manuscript submitted; attached as supplemental materials) ; 2) evaluate the
111 current dosing strategy using simulation analysis; 3) propose a new precision dosing regimen and
112 a Bayesian adaptive control strategy using additional concentration measurements for optimal
113 dosing based on the developed PK model; 4) characterize the relationship between alemtuzumab
114 exposure and lymphocyte depletion by a population PK-PD model in pediatric and young adult
115 patients undergoing HCT.

116

Methods

Patients and sampling

Data were collected from 29 pediatric and young adult patients with non-malignant disorders undergoing HCT enrolled in two studies. Alemtuzumab was administered subcutaneously with fludarabine and melphalan under the designated RIC regimen prior to HCT (Figure S1). Alemtuzumab dosing for Study 1 and Study 2 was as follows:

Study 1 (n = 17): This study was previously reported by our team [4]. Briefly, alemtuzumab was given as a total dose of 1 mg/kg on Days -14 to -10 (Days 14 to 10 before the transplant date). For patients with body weight < 15 kg, the total dose was divided equally over 5 days. For patients with body weight \geq 15 kg, the first dose was limited to 3 mg (the manufacturer's recommended maximum initial dose) and the remainder of the 1 mg/kg total dose was divided over the remaining 4 days. Blood samples were drawn for PK measurement at predose, and 0.5, 2, 4, 6, 8 hours after the first two doses, and 0.5, 8 hours after the 3rd and 4th doses. Daily concentration measurements started from day 5 until graft infusion.

Study 2 (n = 12): This study was approved by the institutional review board and is described and registered at Clinicaltrials.gov (NCT03302754). Informed consent was obtained for all patients. For patients with body weight < 15 kg, alemtuzumab was given as a total dose of 0.6 mg/kg on Days -14 to -12 (0.2 mg/kg/dose). For patients with body weight \geq 15 kg, the first dose was limited to 3 mg and the following doses were approximately 0.23 mg/kg/dose on days -13 and -12 (to equal a total dose of approximately 0.5-0.6 mg/kg). Based on a preliminary PK analysis, [9] patients who were projected to clear alemtuzumab by Day 0 to less than 0.15 μ g/mL received an top-up dose on Day -3 or Day -1. The plasma samples were collected 15 minutes prior to the third dose, 8 and 24 hours following the third dose, and then daily through day 0. Alemtuzumab concentrations in plasma were quantified by a validated flow cytometric assay according to the method previously reported [4].

Population PK-PD modelling

Population PK-PD analysis was performed by nonlinear mixed effect modeling using NONMEM (ICON, Ellicott City, MD, USA). Perl speaks NONMEM (PsN) version 3.6.2 [10] and Pirana version 2.7.1 (Certara USA, Inc., Princeton, NJ, USA) were used as the interface. NONMEM

version 7.4 with the Stochastic Approximation Expectation–Maximization (SAEM) estimation algorithm, followed by important sampling (IMP) method was employed to estimate the typical population parameters, random effect of inter-individual variability, and residual errors simultaneously. The inter-individual variability was assessed using the following model (Equation 1):

$$P_i = P_{pop} \times \exp(\eta_i) \quad (1)$$

where P_i is the estimated parameter value for individual i ; P_{pop} is the typical population value of the PK or PD parameters such as clearance and volume of distribution; η_i is an inter-individual random effect for individual i . The intra-individual variability was described by a proportional error model (Equation 2) or an exponential model (Equation 3).

$$Y_{i,j} = C_{pred,i,j} \times (1 + \varepsilon_i) \quad (2)$$

$$Y_{i,j} = C_{pred,i,j} \times \exp(\varepsilon_{exp}) \quad (3)$$

where $Y_{i,j}$ is the observed concentration, $C_{pred,i,j}$ is the predicted concentration for individual i , and ε is a residual error.

As subcutaneous alemtuzumab absorption has not been quantitatively described, one of our modeling foci was to identify the best absorption model. The following absorption model structures were evaluated: 1) a first order absorption with or without a lag time; 2) a sequential linked or unlinked zero- and first-order absorption [11], and 3) a parallel zero- and first-order absorption processes [8].

For the population PK–PD modeling, both sequential and simultaneous approaches were initially evaluated [12]. The sequential approach eventually was used as it provided non-inferior performance than simultaneous fitting and was much more efficient in computational time (minutes versus hours in running time). PK-PD model structures including direct and indirect linear, inhibitory E_{max} , and sigmoidal E_{max} models were evaluated. ALC counts that were below the limit of quantification (i.e. < 0.01 k/ μ l) were excluded from the analysis as these measurements did not reflect quantitative PK-PD correlation changes.

Covariate analysis

Demographic and laboratory characteristics of the patients including body weight, age, baseline ALC, white blood count (WBC) and albumin levels at start of alemtuzumab treatment, along with daily measured ALC and WBC during the treatment were evaluated as potential covariates using the stepwise selection method. The change in the objective function value (OFV) between two nested models was assumed to follow the χ^2 distribution, and forward inclusion and backward elimination with a significance level of < 0.05 (-3.84 points in OFV) and < 0.01 (-6.64 points in OFV) were used, respectively. In accordance with allometry theory, body weight was found to be significantly correlated to alemtuzumab clearance (CL) and volume of distribution (V) at initially evaluation. We therefore used allometrically scaled body weight to account for differences in body size as follows (Equation 4):

$$P_i = P_{pop} \times \left(\frac{BW_i}{BW_{standard}} \right)^{Power} \quad (4)$$

where BW_i is body weight for individual i , $BW_{standard}$ is 70 kg, and power is the coefficient set at 0.75 for CL and 1 for V. Other potential covariates were tested as formulated to a linear or power function as illustrated using ALC as an example (Equations 5 and 6):

$$P_i = P_{pop} \times \left(1 + \left(\frac{ALC_i}{ALC_{median}} \right) \times l \right) \quad (5)$$

$$P_i = P_{pop} \times \left(\frac{ALC_i}{ALC_{median}} \right)^k \quad (6)$$

where P_i and ALC_i are the parameter and ALC at predose for individual i , ALC_{median} is the standardized value for ALC at predose. The l and k represent the slope and power factor of the relationship, respectively (i.e. Equation 5 and 6 for linear and power relationship equations, respectively).

195

Model evaluation

The following criteria were considered for model selection: successful convergence, objective function value (or Akaike Information Criterion), precision of parameter estimates, and plausibility of parameter estimates. In addition, diagnostic goodness-of-fit plots and graphical assessments were performed using R version 3.6.2 and Xpose version 4.4.0 [13]. The following diagnostic plots were used to evaluate the models: observed value (DV) vs. population predicted

value (PRED), DV vs. individual predicted value (IPRED), conditional weighted residuals vs. PRED and conditional weighted residuals vs. time after dose to identify a bias corresponding to model mis-specification. A non-parametric bootstrap analysis was employed to evaluate the stability of the final model using Perl-speaks-NONMEM (PsN) version 3.5.3. The resampling was done 500 times, and 95% confidence intervals of parameter estimates from the bootstrap analysis were compared to the final model estimates. The prediction-corrected visual predictive check (pcVPC) was used for final evaluation [14]. One thousand replicates of simulated datasets were generated using the final model and the distribution of simulated observations was compared with the actual observations.

Monte Carlo Simulation

Monte Carlo simulation which considers both population average and individual variability, was conducted to select an appropriate dose to achieve a peri-transplant alemtuzumab concentration of 0.15-0.6 µg/mL on the day of transplantation (Day 0). This target range is based on our previous findings on alemtuzumab efficacy and safety for the RIC regimen [4]. A range of candidate cumulative doses based on three dose calculation methods were tested: 1) based on total body weight as mg per kg, as in the current dosing protocol; 2) based on total body weight using the allometric scaling principle: allometric dose = dose for a typical subject of 70 kg x (total body weight/70)^{0.75}; 3) based on body surface area (BSA, mg per m²). The dosing scheme was designed as the total dose divided to 3 equal doses administered on Days -14 to -12 (14 days to 12 days before the transplant date). However, to ensure patient safety, the first dose on Day -14 could not exceed 3 mg. If the calculated first dose was above 3 mg, 3 mg was the set dose on Day -14 and the rest of the dose amount was equally divided to be administered over the remaining 2 days. In subjects with a predicted Day 0 concentration below 0.15 µg/mL, simulation-based individualized top-up dose was administered on Day -3. In the simulation analysis, 1,000 patients aged 0.3-22 years were randomly sampled from the US Centers for Disease Control and Prevention-National Health and Nutrition Examination Survey (CDCNHANES) database. The distribution of the weight – age cohorts from the sampled virtual subjects were plotted to assure similarity to the intended study treatment cohort (Supplemental Figure S2). The percentage of subjects who had a day 0 concentration within the target exposure range was summarized for each dosing regimen. All simulations to determine exposure levels of

233 alemtuzumab associated with candidate dosing regimen were conducted using the R package
234 mrgsolve [15]

235

236 *Statistical Analysis*

237 Student t test was used for the comparison of patient characteristics between top-up and no top-
238 up dose groups. Linear regression analysis was run to understand the correlation between
239 alemtuzumab exposure and patient characteristics. A P value of <0.05 was considered
240 significant.

Results

Population PK modeling

The median age of the study subjects was 6.4 years (range: 0.28-21.4 years) and the median body weight was 32.0 kg (4.3-139 kg). Other patient demographics are summarized in Table 1. For PK modeling, a sequential zero- and first- order input model was found to best describe the alemtuzumab absorption profile after subcutaneous administration. A one-compartment model with first-order disposition adequately described alemtuzumab disposition. A two-compartment model or nonlinear Michaelis-Menten disposition were also evaluated but did not provide significant model improvements. Allometrically scaled body weight was included in the model to account for body size related differences in volume of distribution and clearance with the theoretical values of 1 for volume and 0.75 for clearance. This inclusion resulted in a significant improvement in model fit ($\Delta\text{OFV} = -33.9$, $p < 0.001$). Of note, when the quantitative impact of weight on PK parameters was estimated as a power function as shown in Equation 4, the exponents were estimated as 0.67 for clearance and 1.17 for volume, respectively. Pre-dose absolute lymphocyte count (ALC) was not identified as a significant covariate of clearance ($P > 0.05$), although a trend of negative correlation with alemtuzumab clearance was observed. No effects of age, gender, or albumin levels on alemtuzumab PK were observed. The inter-patient variability of clearance and volume of distribution were high (69.7% and 89.7%, respectively), and the duration of the zero order absorption process was highly variable, with a coefficient of variation (CV) of 225.6%. The population PK parameter estimates are summarized in Table 2. The population clearance estimate was 0.080 L/h/70kg and the volume of distribution estimate was 17.4 L/70kg. Goodness-of-fit plots indicated slight over predictions of high concentrations but showed an overall reasonable model fit (Figure 1A-1D). The non-parametric bootstrap analysis demonstrated stability of the model estimates on clearance and volume of distribution but high variability in absorption parameters (Table 2). The simulated plasma concentrations by VPC analyses were in a reasonable agreement with the observed data. The 10th, 50th, and 90th percentile of predictions overlaid well 0.673 with their corresponding percentile of observations (Figure 2A).

Population PK-PD modeling

A direct inhibitory E_{\max} model defined as shown below best characterized the PK-PD relationship between alemtuzumab concentration and ALC.

$$ALC = E_{\max} * (1 - \text{Conc}/(\text{EC}_{50} + \text{Conc}))$$

where ALC is the absolute lymphocyte count; E_{\max} is the maximum inhibitory effect; EC_{50} is the alemtuzumab concentration when half of the E_{\max} is achieved; Conc represents the alemtuzumab concentration.

This model performed better in terms of overall fit and stability compared to a linear or a sigmoidal E_{\max} model. We also evaluated an indirect response model as described in earlier studies [5, 16], however this model structure was not supported by the data. The population E_{\max} was estimated as $1.27 * 10^3/\mu\text{L}$ and the EC_{50} was $0.06 \mu\text{g/mL}$. The observed inter-individual variability for E_{\max} was 85 % and was 131% for EC_{50} . E_{\max} and EC_{50} are correlated with a correlation coefficient of -0.7. Other final model parameters are presented in Table 2. Goodness-of-fit plots indicated some over-prediction at the population level but was acceptable at the individual level (Figure 1E-1H). Further model evaluation by bootstrap indicated that the model was stable and all parameter estimates were within less than 10% different from the population median levels (Table 2). The VPC plot showed that the model predictions overall were adequate but trended higher than observations after 200 hours. As alemtuzumab concentrations decreased, ALC remained low (Figure 2B).

Dose optimization to achieve optimal target exposure on the day of transplantation (Day 0)

The current off-label use of alemtuzumab in pediatric patients is based on per kg dosing, which assumes a linear relationship between body weight and drug elimination/metabolism. In our pilot study (n = 12), we observed that this per kg dosing results in an uneven alemtuzumab exposure across different age/weight spectra (Figure S3). In patients who needed an additional top-up dose of alemtuzumab, body weight and age were significantly lower than in subjects who did not require a top up dose (Figure S3 A&B, $p < 0.05$). In addition, alemtuzumab exposure on Day -5 was moderately correlated with age and body weight, with lower concentrations in the young/low weight patients and higher concentrations in the older/higher weight patients (Figure S3 C&D).

300 In light of this non-proportional correlation between alemtuzumab exposure with the per kg
301 dosing and the allometric scaling applied in the population PK models, we conducted simulations
302 to identify optimal starting dose with three dose calculation methods: 1) allometrically scaled
303 dosing (individual dose = dose for a typical subject of 70 kg x (individual weight/70)^{0.75}), 2)
304 BSA-based dosing (mg per m²) and 3) body weight-based dosing (mg per kg). The PK profiles
305 with candidate doses were simulated and the mean alemtuzumab concentrations with 10th – 90th
306 percentile of confidence intervals were evaluated in achieving the target concentrations of 0.15-
307 0.6 µg/mL on Day 0. As shown in Figures 3A, S4A and S5, alemtuzumab PKs show large inter-
308 patient variability with broad prediction intervals with all three dosing methods. Per kg dosing
309 would result in uneven alemtuzumab exposure across different age spectra, whereas BSA- or
310 allometry-based dosing showed overall similar exposure levels in different age groups (Figure
311 4). For allometry-based dosing, a dose level of 18 mg*(WT/70)^{0.75} would have the highest
312 percentage of virtual patients (56.6%) achieving the ideal therapeutic range of 0.15-0.6 µg/mL
313 on Day 0 (Table 3). For BSA-based dosing, the dose level associated with the highest
314 percentage of target attainment was 10 mg/m² (56.5%) (Table 3). Simulation analysis further
315 indicated that in patients with a predicted alemtuzumab plasma concentration lower than the
316 targeted 0.15 µg/mL, a top-up dose of 7 mg*(WT/70)^{0.75} for allometry-based dosing or 3.7 mg/m²
317 for BSA-based dosing on Day -3 would bring the alemtuzumab concentration to the optimal
318 range on Day 0 in 27.2% and 26.0% additional patients, respectively (Figures 3B & S4B).

319

Discussion

Our group previously reported the effect of alemtuzumab concentration on Day 0 (transplant day) on allogeneic HCT outcomes and identified an ideal therapeutic range of 0.15-0.6 $\mu\text{g/mL}$ [4]. A recent follow-up prospective pilot study however demonstrates that a reduced dosing schedule (cumulative dose of 0.5-0.6 mg/kg) is still too high in more than 40% of patients (manuscript submitted; attached as supplemental materials). Further dose de-escalation along with continued adaptive dose controls would be required to bring the majority of the patients into the proposed target range to prevent acute GVHD and to reduce the risk of mixed chimerism and delayed early post-HCT immune recovery. The current study characterized the population PK and PK-PD of alemtuzumab and conducted trial simulations with different dosing scenarios to identify the initial dose level for dose de-escalation. Based on the result, we propose consideration of a new dosing scheme for alemtuzumab which could be imbedded in a Bayesian algorithm for precision dosing as shown in Figure 5 and tested in a future trial.

The current PK modeling practice advanced our preliminary analysis[9], and found that alemtuzumab PK could be best described by a one-compartment model with a zero- and first – order absorption, and first order elimination. The performance of this one-compartment model was non-inferior compared to a two-compartment model or a nonlinear Michaelis-Menten model as described by other studies for alemtuzumab PK [5, 7]. The disparity between studies could be due to different administration routes, and dose levels, and PK sampling schemes. As a large antibody of 150-kDa, alemtuzumab is mostly confined in the plasma and interstitial space [17]. After subcutaneous administration, the slow absorption to the central compartment (i.e. blood circulation) may limit alemtuzumab distribution to the extravascular space. In addition, our study subjects received relatively low doses (maximal single dose was 30 mg or 0.24 mg/kg) whereas in the adult study the maximal dose was 240 mg (approximately 3.3 mg/kg) [5]. This may explain why our data did not support a nonlinear Michaelis-Menten model. The estimated apparent clearance (CL/F) in our analysis is 0.080 L/h/70kg. Considering a reported bioavailability of 47% after subcutaneous alemtuzumab [17], the absolute clearance would be calculated as 0.038 L/h/70kg which is comparable to the clearance reported in a recent pediatric study (approximately 0.05 L/h/70kg) [7].

Pre-dose ALC values showed a trend of negative correlation with alemtuzumab clearance in our analysis, but did not reach statistical significance. An earlier pediatric study also did not identify significant impact of baseline lymphocytes on alemtuzumab clearance [7]. However, we did find that alemtuzumab concentrations at Day 0 negatively correlated with pre-dose ALC ($R^2 = 0.68$; [4]), which is not surprising as high ALC counts should increase target-mediated drug disposition and high alemtuzumab concentrations should cause more lymphocyte depletion. Future larger-scale studies will help to further delineate the association between baseline ALC and alemtuzumab clearance. Alemtuzumab clearance may also be affected by the formation of anti-alemtuzumab antibodies [18]. Careful attention to this will be required in the future.

The PK-PD relationship of alemtuzumab was evaluated using ALC counts as the PD marker in this study. Consistent with previous studies, we observed an immediate and almost complete ALC depletion after alemtuzumab treatment despite a wide range of initial ALC counts (0.06 – 6.52 k/ μ L). The developed population model includes an inhibitory E_{\max} model. The estimated E_{\max} of 1.27 k/ μ L equals the median value of baseline ALC, indicating the capability of a complete lymphocyte depletion. A relatively low mean EC_{50} of 0.062 μ g/mL confirms a high potency of alemtuzumab to reduce the number of lymphocytes. For WBC depletion in adult patients with chronic lymphocytic leukemia, the estimated EC_{50} value is much higher (0.306 μ g/mL) [5], which is not unexpected as CD52 + cells are only part of all WBC. Similar to the high variability associated with PK parameters, PD parameters also exhibit large inter-patient variability. The CV% for E_{\max} was 85% and CV% for EC_{50} was over 100%. One of the limitations of this PK-PD modeling analysis is the lack of PK and PD data during the first 48 hours after the start of alemtuzumab treatment. In almost all subjects, ALC counts dropped to a minimum level within 48 hours, therefore the impact of alemtuzumab exposure on ALC count during this 48 hours interval could not be evaluated. However, this PK-PD model represents a first attempt to quantitatively describe the PK-PD relationship of alemtuzumab in children and young adults, and provides a potential pathway for future development of a PD-guided dosing strategy for alemtuzumab therapy.

Currently, alemtuzumab is used off-label in pediatric patients and the dosing strategy is based on body weight (per kg). Our recent clinical study indicated that in almost half of the patients, a reduced alemtuzumab dosing of 0.5-0.6 mg/kg resulted in a Day 0 concentration above the target range (manuscript submitted; attached as supplemental materials). We further found that the

current per kg dosing protocol for children and young adults may not accurately reflect the nonlinear relationships between body mass and alemtuzumab pharmacokinetics: in our pilot study, per kg dosing caused in general lower drug exposure in younger/lower weight patients and higher exposure in older/higher weight patients. We therefore considered allometrically scaled- and BSA-based dosing in addition to the per kg dosing in our clinical trial simulation study. Consistent with clinical observations, simulated alemtuzumab concentrations under per kg dosing were not equal across different age and body weight cohorts. Figure S6 illustrates the predicted dose levels with all three dose calculation approaches. Compared to allometric dosing centered to 70 kg or BSA-based dosing, the linear per kg dosing would result in a slightly lower alemtuzumab dose for patients weighing less than 70 kg and a higher dose for patients weighing more than 70 kg. Because allometric dosing could accurately reflect the non-linear correlation between body size and clearance as identified in the population PK model, it has the potential to optimize alemtuzumab therapy for patients of all weights and ages. BSA-based dosing can also be considered for ease of clinical use given that allometric dosing is not widely used in clinical practice. The clinical outcome (efficacy and safety) of this newly proposed dosing scheme, however, remains to be confirmed. We plan to conduct a prospective clinical trial to further study target attainment with this new model-informed precision dosing scheme. For patients with a predicted Day 0 level below the target alemtuzumab plasma concentration ($0.15 \mu\text{g/mL}$), we propose to consider an average top-up dose ($7 \text{ mg} \cdot (\text{WT}/70)^{0.75}$ (or 3.7 mg/m^2) based on allometry or BSA, respectively) to bring the concentrations up to target. However, if Bayesian estimation are applied, a simulation can be conducted at the individual level and a precision top-up dose can be estimated for each patient similar to our previous study [3].

In summary, we report a population PK-PD model of alemtuzumab after subcutaneous administration in pediatric and young adult transplant patients. Our modeling and simulation analyses suggest that an initial dose level of $18 \text{ mg} \cdot (\text{WT}/70)^{0.75}$ (or 10 mg/m^2) divided over 3 days combined with a Bayesian adaptive dosing strategy would result in a better alemtuzumab target exposure attainment in pediatric patients undergoing allogeneic HCT. Further clinical studies are warranted to evaluate the efficacy and safety of this newly proposed dosing scheme.

410 Reference

- 411 1. Guilcher GMT, Shah R, Shenoy S. Principles of alemtuzumab immunoablation in hematopoietic
412 cell transplantation for non-malignant diseases in children: A review. *Pediatr Transplant* 2018; 22.
- 413 2. Marsh RA, Lane A, Mehta PA, Neumeier L, Jodele S, Davies SM, Filipovich AH. Alemtuzumab
414 levels impact acute GVHD, mixed chimerism, and lymphocyte recovery following alemtuzumab,
415 fludarabine, and melphalan RIC HCT. *Blood* 2016; 127: 503-12.
- 416 3. Fukuda T, Emoto C, Marsh RA, Neumeier L, Vinks AA, Mehta PA. Precision Dosing of
417 Alemtuzumab: Population Pharmacokinetic Modeling in Pediatric Patients Undergoing Allogeneic
418 Hematopoietic Cell Transplantation for Non-Malignant Diseases. *Blood* 2016; 128: 2203.
- 419 4. Marsh RA, Fukuda T, Emoto C, Neumeier L, Khandelwal P, Chandra S, Teusink-Cross A, Vinks AA,
420 Mehta PA. Pretransplant Absolute Lymphocyte Counts Impact the Pharmacokinetics of Alemtuzumab.
421 *Biol Blood Marrow Transplant* 2017; 23: 635-41.
- 422 5. Mould DR, Baumann A, Kuhlmann J, Keating MJ, Weitman S, Hillmen P, Brettman LR, Reif S,
423 Bonate PL. Population pharmacokinetics-pharmacodynamics of alemtuzumab (Campath) in patients with
424 chronic lymphocytic leukaemia and its link to treatment response. *Br J Clin Pharmacol* 2007; 64: 278-91.
- 425 6. Dong M, Mizuno T, Vinks AA. Opportunities for model-based precision dosing in the treatment
426 of sickle cell anemia. *Blood Cells Mol Dis* 2017; 67: 143-47.
- 427 7. Admiraal R, Jol-van der Zijde CM, Furtado Silva JM, Knibbe CAJ, Lankester AC, Boelens JJ, Hale G,
428 Etuk A, Wilson M, Adams S, Veys P, van Kesteren C, Bredius RGM. Population Pharmacokinetics of
429 Alemtuzumab (Campath) in Pediatric Hematopoietic Cell Transplantation: Towards Individualized Dosing
430 to Improve Outcome. *Clin Pharmacokinet* 2019; 58: 1609-20.
- 431 8. Kagan L. Pharmacokinetic modeling of the subcutaneous absorption of therapeutic proteins.
432 *Drug Metab Dispos* 2014; 42: 1890-905.
- 433 9. Fukuda T, Emoto C, Marsh RA, Neumeier L, Vinks AA, Mehta PA. Precision Dosing of
434 Alemtuzumab: Population Pharmacokinetic Modeling in Pediatric Patients Undergoing Allogeneic
435 Hematopoietic Cell Transplantation for Non-Malignant Diseases *Blood* 2016; 128: 2203.
- 436 10. Lindbom L, Ribbing J, Jonsson EN. Perl-speaks-NONMEM (PsN)--a Perl module for NONMEM
437 related programming. *Comput Methods Programs Biomed* 2004; 75: 85-94.
- 438 11. Holford NH, Ambros RJ, Stoeckel K. Models for describing absorption rate and estimating extent
439 of bioavailability: application to cefetamet pivoxil. *J Pharmacokinet Biopharm* 1992; 20: 421-42.
- 440 12. Zhang L, Beal SL, Sheiner LB. Simultaneous vs. sequential analysis for population PK/PD data I:
441 best-case performance. *J Pharmacokinet Pharmacodyn* 2003; 30: 387-404.
- 442 13. Jonsson EN, Karlsson MO. Xpose--an S-PLUS based population
443 pharmacokinetic/pharmacodynamic model building aid for NONMEM. *Comput Methods Programs*
444 *Biomed* 1999; 58: 51-64.
- 445 14. Bergstrand M, Hooker AC, Wallin JE, Karlsson MO. Prediction-corrected visual predictive checks
446 for diagnosing nonlinear mixed-effects models. *AAPS J* 2011; 13: 143-51.
- 447 15. Elmokadem A, Riggs MM, Baron KT. Quantitative Systems Pharmacology and Physiologically-
448 Based Pharmacokinetic Modeling With mrgsolve: A Hands-On Tutorial. *CPT Pharmacometrics Syst*
449 *Pharmacol* 2019; 8: 883-93.
- 450 16. Li Z, Richards S, Surks HK, Jacobs A, Panzara MA. Clinical pharmacology of alemtuzumab, an anti-
451 CD52 immunomodulator, in multiple sclerosis. *Clin Exp Immunol* 2018; 194: 295-314.
- 452 17. van der Zwan M, Baan CC, van Gelder T, Hesselink DA. Review of the Clinical Pharmacokinetics
453 and Pharmacodynamics of Alemtuzumab and Its Use in Kidney Transplantation. *Clin Pharmacokinet*
454 2018; 57: 191-207.

455 18. Baker D, Ali L, Saxena G, Pryce G, Jones M, Schmierer K, Giovannoni G, Gnanapavan S, Munger
456 KC, Samkoff L, Goodman A, Kang AS. The Irony of Humanization: Alemtuzumab, the First, But One of the
457 Most Immunogenic, Humanized Monoclonal Antibodies. *Front Immunol* 2020; 11: 124.

458

459

460 **Tables:**

461 **Table 1** Summary of demographics

	Age (Year)	BW (kg)	ALC (k/ μL) [†]	WBC (k/ μL)	Diagnosis
Study 1	N= 17				HLH (n=10), CGD (n=2), IPEX (n=2), aplastic anemia (n=1), CID (n=1), SCID (n=1)
Median	7.0	32.2	1.03	7.1	
Min	0.5	8.92	0.06	0.4	
Max	18.0	91.5	6.0	12.5	
Study 2	N= 12				HLH (n=3), SAA (n=3), PNH (n=1), Glanzmann's (n=1), Kostmann's syndrome (n=1), idiopathic aplastic anemia (n=1), erythropoietic protoporphyrria (n=1), leaky SCID (n=1)
Median	5.4	23.3	2.28	3.9	
Min	0.28	4.32	0.53	1.0	
Max	21.4	139	6.52	9.1	
Total	N= 29				
Median	6.4	32.0	1.27	4.1	
Min	0.28	4.32	0.06	0.4	
Max	21.4	139	6.52	12.5	

462 HLH, hemophagocytic lymphohistiocytosis; CGD, chronic granulomatous disease; IPEX, immunodysregulation,
463 polyendocrinopathy, enteropathy, X-linked; CID, combined immune deficiency; SCID, severe combined immune
464 deficiency; SAA, severe aplastic anemia

465

466 **Table 2** Population pharmacokinetic parameter estimates

Parameters (units)	Estimates	RSE (%)	Bootstrap estimates	
			Median	95% CI
Fix-effect parameters				
CL/F (L/h/70kg)	0.0795	14.5	0.0799	0.061-0.103
V/F (L/70kg)	17.4	17.3	17.0	5.8- 25.2
k _a (/h)	0.079	26	0.094	0.032-1.774
Duration for zero order absorption (h)	6.77	51	8.67	1.71-46.44
E _{max} (k/μl)	1.27	18.7	1.30	0.88-1.93
EC ₅₀ (μg/ml)	0.062	27.3	0.059	0.032-0.108
Inter-patient variability (CV%)				
IIV _{CL}	67.7	17.3	67.8	42.0-93.2
IIV _V	62.5	15.4	83.6	0.09-227.1
IIV _{Ka}	101	20.2	109	0.05-353.2
IIV _{DUR}	183	19.1	193	66.6-322.4
IIV _{E_{max}}	85	22.3	77	22-106
IIV _{EC50}	131	23.4	123	70-172
Correlation of E _{max} – EC ₅₀	-0.75	23.9	-0.62	(-1.21)-(-0.09)
Residual variability				
Prop.Err.Conc (CV%)	39.8	3.8	39.3	29.7-48.2
Add.Err.Effect (k/μl)	0.01	41	0.00	-0.07-0.09
Prop.Err.Effect (CV%)	68.9	6.7	68.0	-0.76-0.88

467 Clearance (CL/F) and volume of distribution (V/F), which are allometrically size-standardized with a power of 0.75
468 and 1.00, respectively; Dur, Duration for zero order absorption; RSE, relative standard error; CI, confidence
469 interval; IIV, inter-individual variability; CV, coefficient of variation; Prop.Err.Conc, proportional part of the
470 residual unexplained variability for alemtuzumab concentrations; Add.Err.Effect, additive part of the residual
471 unexplained variability for ALC count; Prop.Err.Effect, proportional part of the residual unexplained variability for
472 ALC count

473 **Table 3 Day 0 target achievement of candidate dosing regimens**

Cumulative dose	Average Day 0 concentration (µg/ml)	Above 0.6 µg/ml (%)	Within 0.15 – 0.6 µg/ml (%)	Below 0.15 µg/ml (%)
Per KG dosing				
0.3 mg/kg	0.26	7.6	54.0	38.4
0.4 mg/kg	0.33	15.7	52.6	31.7
0.5 mg/kg	0.45	28.9	45.2	25.9
0.6 mg/kg	0.56	38.5	38.6	22.9
Per BSA dosing				
8 mg/m ²	0.24	5.4	54.7	39.9
10 mg/m ²	0.31	11.7	56.5	31.8
12 mg/m ²	0.36	16.8	56.3	26.9
14 mg/m ²	0.43	26.0	49.0	25.0
Allometry-based dosing				
16 * (WT/70) ^{0.75}	0.25	7.2	55.3	37.5
18 * (WT/70) ^{0.75}	0.28	9.1	56.6	34.3
20 * (WT/70) ^{0.75}	0.31	13.7	54.2	32.1
22 * (WT/70) ^{0.75}	0.34	16.4	53.5	30.1

474

475

Figure legends:

Figure 1 Goodness-of-fit plots for the final model.

A-D: Goodness-of-fit plots for the final PK model. E-H: Goodness-of-fit plots for the final PK-PD model. (A & E) Population prediction vs. observations. (B & F) Individual prediction vs. observations. (C & G) Conditional weighted residuals (CWRES) vs. population prediction. (D & H) Conditional weighted residuals (CWRES) vs. time after dose. Solid line, unity line (for A,B,E,F, linear regression with a slope=1, for C,D,E,F, line of identity showing zero). Red line, local regression line.

Figure 2 Visual predictive check of the final population PK (A) and PK-PD (B) model

Circles: observed plasma concentrations; red dashed lines: observed 10th and 90th percentile; red solid line: observed median; shaded areas, confidence intervals around the 10th, 50th and 90th percentile predictions.

Figure 3 Monte Carlo simulation of allometry-based dosing regimens.

(A) Simulated alemtuzumab PK profiles with a cumulative dose of 16 mg*(WT/70kg)^{0.75}, 18 mg*(WT/70kg)^{0.75}, 20 mg*(WT/70kg)^{0.75} or 22 mg*(WT/70kg)^{0.75} divided to three doses. (B) For patients who had a Day 0 concentration below 0.15 µg/mL, a top-up dose of 7 mg*(WT/70kg)^{0.75} administered on Day -3 would bring most of patients to the exposure target range. The red lines represent predicted mean concentrations and the shaded areas indicate the 10 percentile to 90 percentile prediction intervals. The grey dashed lines shows the target of 0.15 – 0.6 µg/ml.

Figure 4 Simulation projected alemtuzumab concentration on Day 0 across different ages.

Note per kg dosing would result in uneven alemtuzumab exposure across different age spectra, whereas BSA- or allometry-based dosing showed overall similar exposure levels in different age groups

Figure 5 Proposed alemtuzumab precision dosing inbeded with Bayesian estimation. This

figure illustrates the proposed alemtuzumab precision dosing strategy. Following initial drug

505 administrations on Day -14 to Day -12, alemtuzumab concentrations are measured and used for
506 Bayesian estimation on Day -5 for a possible additional dose selection to achieve a target
507 concentration of 0.15 - 0.6 µg/ml. The dashed line represents the model predicted alemtuzumab
508 PK profile in a typical subject. The red dots represent measured alemtuzumab concentrations.
509 The solid line represents the Bayesian estimated individual PK profile including the predicted
510 increase in concentration after the additional dose. Note that if no top-up dose was given, the
511 projected Day 0 concentration would be below the target.

512 **Figure 1**

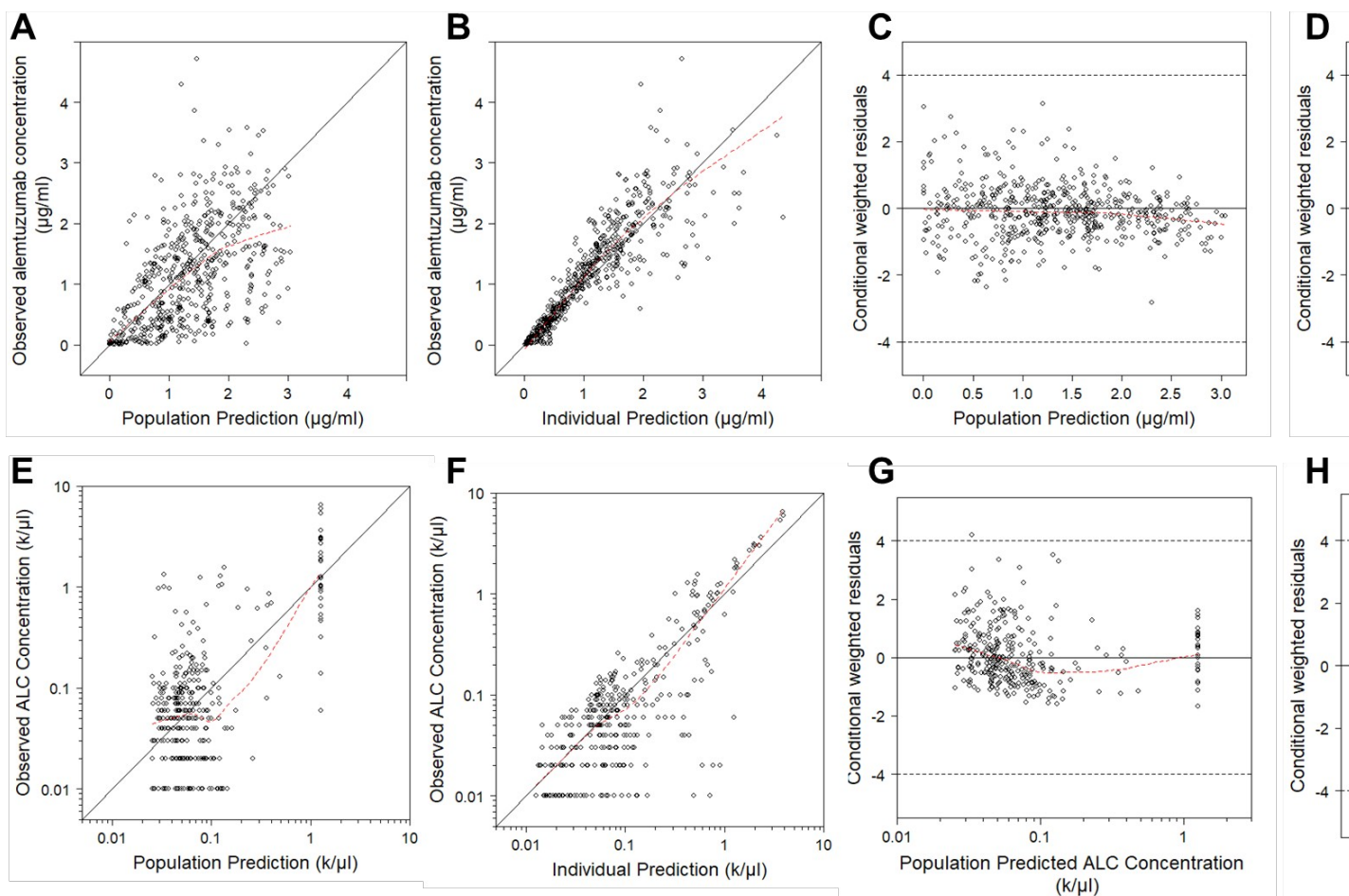
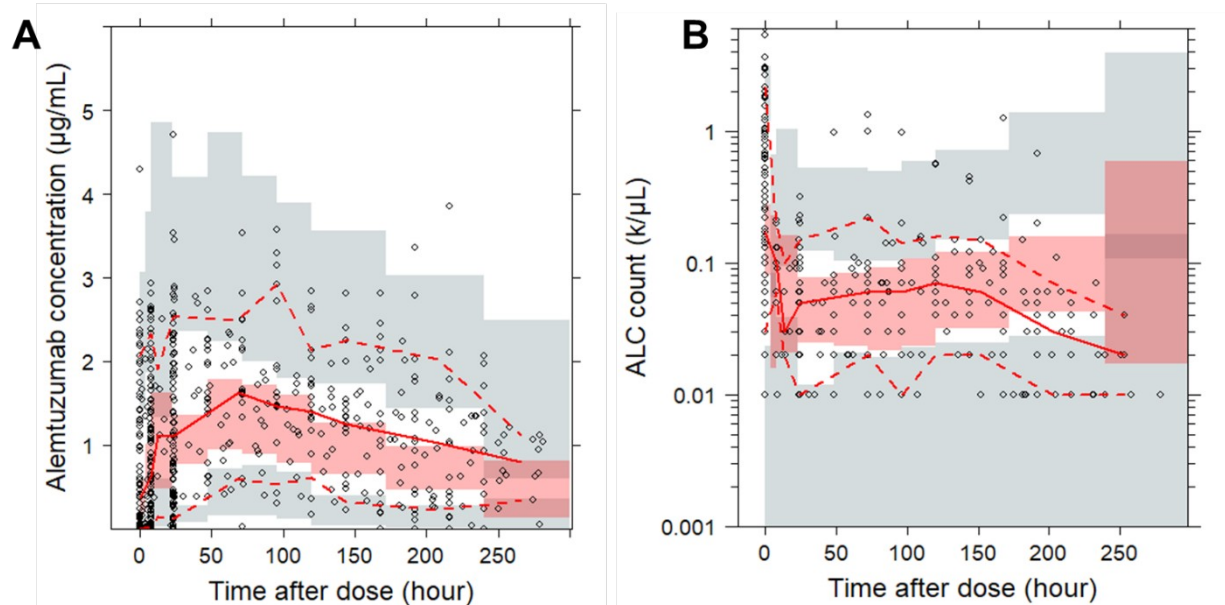
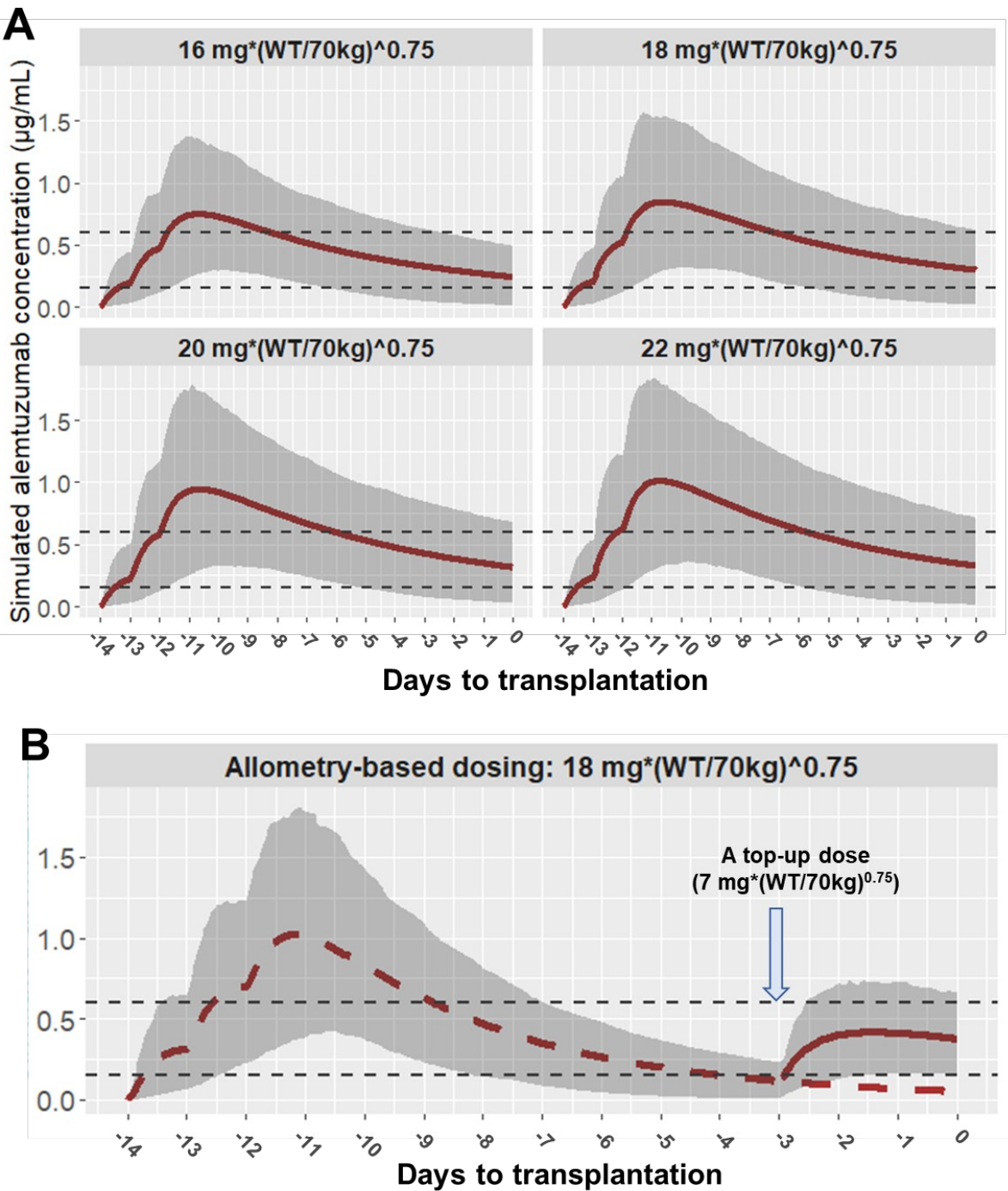


Figure 2



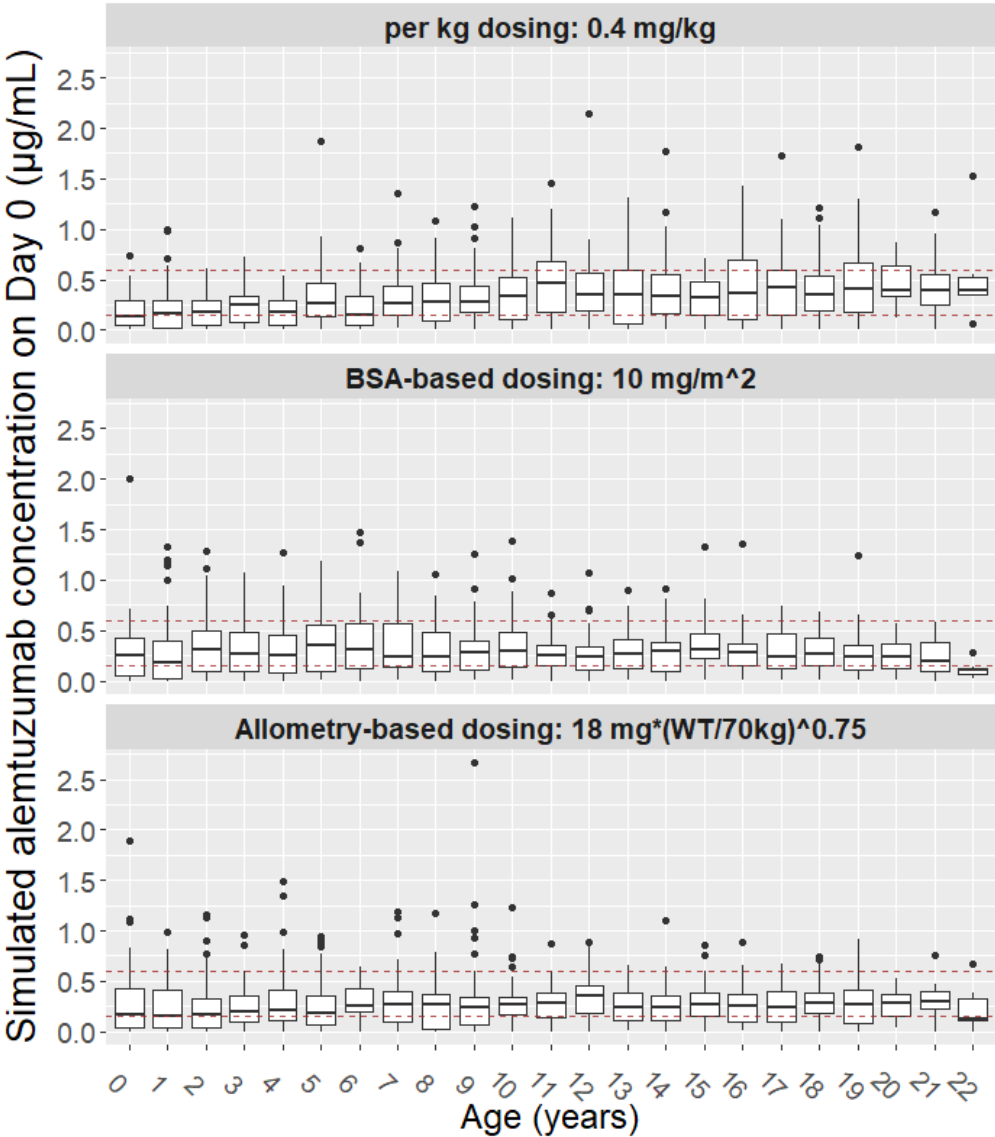
517 **Figure 3**



518

519

520 **Figure 4**



521

522

